Phys Chem Minerals (2001) 28: 746–755

ORIGINAL PAPER

M. H. Müser · K. Binder

Molecular dynamics study of the α–β transition in quartz: elastic properties, finite size effects, and hysteresis in the local structure

Received: 8 September 2000 / Accepted: 2 July 2001

Abstract The α–β transition in quartz is investigated by molecular dynamics simulations in the constant stress ensemble. Based on a frequently used two-body interaction potential for silica, it is found that anomalies in the elastic constants are at least in semiquantitative agreement with experiment despite the fact that no anomaly in the c/a ratio is observed in the simulations. A finite-size scaling analysis shows that first-order Landau theory is applicable to the employed model potential surface. This statement also applies to the susceptibility below the transition temperature T_{tr}, which has not yet been measured experimentally. Examination of the local order near T_{tr} reveals that the deformation of SiO_4 tetrahedral units is equally large in the β phase as in the α phase. However, large hysteresis effects can be observed in the local structure for distances $r > 4$ Å. The results are in agreement with the picture of a first-order displacive phase transformation which is driven by the motion of deformed tetrahedral SiO_4 units. Yet, the fast oscillations of oxygen atoms are around (time-dependent) positions that do not correspond to the ideal oxygen positions in β-quartz. The averaged configurations resemble the ideal structure only if averaged over at least a few nanoseconds.

Key words Molecular dynamics model · Finite-size effects · Landau Theory

Introduction

The nature of the α–β transition in quartz and other silica polymorphs has been the subject of long controversy (Dolino 1990; Heaney et al. 1994; Carpenter et al. 1998; Demuth et al. 1999; Dove et al. 1999). It is often discussed in terms of the real structure of β-quartz. If β-quartz consisted of α_1 and α_2 domains, which spatially and dynamically averaged to the idealized β-quartz structure, then the phase transformation could be expected to be an order–disorder transition. Neutron diffraction (Wright and Lehman 1981), NMR studies (Spearing et al. 1992), and molecular-dynamics simulations (Tsuneyuki et al. 1990) were interpreted as evidence for this scenario. The majority of recent studies, however, favors a displacive type of phase transformation. In this case, the actual structure of the high-temperature phase is interpreted as an ideal β-quartz structure, which is distorted by rigid unit modes (RUM) of relatively stiff tetrahedral SiO_4 units. This point of view explains the existence of soft modes in the α and β phases (Axe and Shirane 1970; Tezuka et al. 1991; Carpenter et al. 1998; Dove et al. 1999) and the absence of symmetry forbidden phonons in the β phase of quartz (Salje et al. 1992). A refined X-ray study of the β-quartz structure also favored an ordered structure, although the oxygen probability density functions (pdf) were seen to deviate considerably from Gaussians (Kihara 1990). The non-Gaussian behavior was not interpreted as disorder but as librational motion of the oxygen atoms around the Si–Si lines. In the following discussion, we will mostly disregard the intermediate incommensurate phase, which has been observed in a relatively small temperature range of 1.5 K (Dolino 1990).

Recent molecular dynamics simulations (MDS) of cristobalite and quartz (Gambhir et al. 1999) focused on the importance of RUMs for the nature of the disorder in the high-symmetry phase of these silica polymorphs. In the simulations the stiffness, s, of SiO_4 tetrahedra was increased artificially. For cristobalite, no localization of the oxygen position on preferred positions was observed even for large values of s. The large number of RUMs in cristobalite was made responsible for the disorder in the high-temperature phase. Unlike β-cristobalite, the oxygen atoms in β-quartz were seen to localize when s was increased. When all modes but the RUMs were frozen, β-quartz ordered. A subsequent theoretical treatment (Dove et al. 1999) of the phase transition in quartz in

M. H. Müser · K. Binder (✉)
Institut für Physik, WA 331,
Johannes Guntenberg-Universität 55099 Mainz, Germany
e-mail: martin.mueser@uni-mainz.de

terms of a so-called coupled ϕ^4 model (Cowley and Bruce 1980) was nevertheless based upon the idea that the β phase of quartz can distort to the α phase through the rotation of RUMs. Semiquantitative agreement in the transition temperature was found with experiment and computer simulations (Tsuneyuki et al. 1990) which were based on a potential energy surface giving some input into the ϕ^4 theory as well.

Another recent study (Carpenter et al. 1998) successfully linked a sophisticated Landau theory for first-order phase transition with excess thermodynamic properties and elastic constant variations associated with the α–β phase transition. Unlike the above-mentioned ϕ^4 theory, the Landau theory went to high orders in the order parameter ϕ and included coupling between stress and ϕ. The coefficients of the Landau theory, however, were not derived from microscopic interaction potentials and no final statement could be made about the mechanism that drives the phase transition. While the ϕ^4 theory and the Landau theory support the idea of a displacive transition, the nature of the disorder in the β phase still remains unclear. In particular, it is unresolved why, on one hand, one potential energy surface seemingly favors the disorder–order point of view when employed in MDS (Tsuneyuki et al. 1990) and, on the other hand, the same potential energy surface supports the idea of a displacive transition when used as an input for the ϕ^4 theory.

While molecular dynamics simulations have been widely used to interpret the phase transition in quartz and other silica polymorphs, some important issues have not yet been addressed: (1) Do the model potentials describe silica well enough to capture the anomalies associated with the transition? So far, it has been shown that the temperature dependence of the volume V and the order parameter ϕ show good agreement with experiment (Tsuneyuki et al. 1990). It has nevertheless never been established that the important anomalies in the elastic constants and in the c/a ratio are reflected in the simulations. This cannot be taken for granted, e.g., the pressure dependence of the elastic constants predicted by simulations and local-density functional theory (Binggeli and Chelikowsky 1992) differ from those measured experimentally (Gregoryanz et al. 2000). (2) There has not yet been a finite-size scaling study making sure that the phase transformation is first order as in the real system. Such a study could address the speculation whether the first-order nature of the transition arises due merely to the incommensurate instability that occurs at a temperature which is 1.5 K higher than the transition into the α-phase. This incommensurate phase will be strongly suppressed in simulations due to finite sizes. A proper analysis of the size dependence of the various moments of ϕ is, furthermore, the only way to determine properly the location of the transition, e.g., it is the only way to determine the phase-transition temperature for fixed pressure and fixed model potential. Alternatively, the phase transition can be induced by varying the stiffness s of tetrahedral SiO_4 units in a computer simulation and again a size scaling should be done in order to assess at what value of s the transition takes place. Calculating expressions of the form $\langle\phi\rangle$ for *finite* systems (as frequently done) only helps us to notice whether or not the simulations are carried out (much) longer than the longest intrinsic relaxation times which typically are due to critical slowing down and/or finite free-energy barriers in the system. (3) No information exists about to what extent SiO_4 units actually do deform at the transition. This information is hard to retrieve from experiment but easy to obtain from simulations. More general, there has been little analysis on how the *local* structure changes when α-quartz transforms to β-quartz upon a temperature variation. Such an analysis is especially interesting in the vicinity of a first-order transformation, where the ordered phase and the disordered phase are (meta)stable for the same thermodynamic parameters.

In this paper, we intend to address these three open issues. This is done by carrying out simulations at constant temperature and zero external stress. For most simulations, the BKS potential (van Beest et al. 1990) was used. The BKS potential has the same functional form as the TTAM potential (Tsuneyuki et al. 1988) which has been used among others by Tsuneyuki et al. (1990) and Gambhir et al. (1999). Typically, BKS gives a somewhat better agreement with experiment than TTAM (Tse and Klug 1991), although the differences are usually quantitative and not qualitative. Of course, it is never expected that classical potentials between the ions describe a real material perfectly well: but if the model reproduces the lattice parameters, elastic constants, etc. within a reasonable approximation, it is safe to draw qualitative conclusions about properties which are easily accessible in the simulation, but not as easily accessible experimentally. There are two reasons why the calculation of elastic constants is crucial to test whether the model describes the α–β transition well: (a) Elastic constants are very sensitive to small changes in the model potential energy surface and (b) they show distinct features at the α–β transition in quartz, as discussed recently and most thoroughly by Carpenter et al. (1998). Of course, it is also important to reproduce the characteristics of the experimentally observed temperature dependence of the order parameter. It is well established that it can be described by the standard Landau expansion for a first-order transition (Grimm and Dorner 1975; Bachheimer and Dolino 1975; Banda et al. 1975). It still needs to be shown that this is also true for the models used in MDS. In order to make predictions for the thermodynamic limit from computer simulations at a phase transition, it is necessary to study systematically the finite-size behavior of various moments of the order parameter (Binder and Stauffer 1987). Once the connection between simulation and experiment is made, it is possible to obtain detailed atomistic information from the simulation. Radial distribution functions $g(r)$ and bond angle distribution functions are well-suited tools to study the instantaneous order in solids. While

these properties are easily accessible in simulations, this is not the case in experiments, where (generalized) radial distribution functions typically have smaller resolution than data relating to the average structure. Moreover, the simulations allow us to measure $g(r)$ for individual chemical species separately, e.g., $g_{\mathrm{SiSi}}(r)$, $g_{\mathrm{SiO}}(r)$, and $g_{\mathrm{SiO}}(r)$. It is difficult to extract this information from experiment if, for example $g_{\mathrm{SiSi}}(r)$ and $g_{\mathrm{OO}}(r)$ overlap in the region of interest.

The molecular dynamics model

Classical molecular dynamics are employed in the constant stress ensemble using the Rahman–Parrinello method (Parrinello and Rahman 1980) for maintaining zero external stress at constant temperature. Elastic constants are calculated exploiting the relation between strain fluctuations and elastic constants (Parrinello and Rahman 1982). The so-called BKS potential energy surface (van Beest et al. 1990) is employed for all simulations, with the slight modification that the short-range (non-Coulombic) interactions are cut off at a distance $r_c = 9.5$ Å.

In order to speed up calculations, interactions and forces were tabulated on a grid with a resolution of 5×10^{-4} Å. No significant differences between simulations using the tabulated and the non-tabulated interactions could be detected. The geometry of our default system containing $N = 1080$ atoms is orthorhombic with box lengths of $A = 25.0$ Å, $B = 26.0$ Å, and $C = 22.1$ Å with A, B, C, parallel to the crystallographic axes a, b, c, respectively. Sometimes, system sizes $N = 2160$ and $N = 4320$ are considered as well, with $A = 30.0$ Å, $B = 34.7$ Å, $C = 27.6$ Å and $A = 40.0$ Å, $B = 43.3$ Å, $C = 33.2$ Å, respectively.

In order to obtain information about the order in the system, a global order parameter ϕ is defined that measures the rotation of (distorted) tetrahedra about the [100] axis, such that

$$\phi = \frac{1}{N^*} \sum_{i^*=1}^{N^*} \varphi_{i^*} \quad , \tag{1}$$

where the sum over i^* is confined to sites which are equivalent to the sites marked by an arrow in Fig. 9. φ_i^* denotes the (averaged) deviation of the orientation in the y–z plane of the (four) Si–O bond(s) from the value in the ideal β-quartz structure.

Thermal expansion and elastic properties

The first check of our model consists of calculating the temperature dependence of the volume. The temperature is lowered in increments of mostly $\Delta T = 150$ K or $\Delta T = 50$ K near the phase transition. One run typically consists of 200×10^3 MD steps adding up to a net time of 200 ps. Correlation times for the $N = 1080$ system do not exceed 5 ps so that one is on the safe side if the first 10 ps are discarded for equilibration. The results are shown in Fig. 1. Inserted are quantum-mechanical calculations based on path-integral molecular dynamics, which are described in detail elsewhere (Müser 2001). The relative difference between simulation (classical MD) and experiment is only about 3%, as could be expected from previous studies employing the BKS potential (van Beest et al. 1990; Tse and Klug 1991). This is a little less than half of the 7% difference between the TTAM potential used in Tsuneyuki et al. (1990) and experiment. It is interesting to note that even if the model potential is perfect, a real agreement between experiment and simulation down to low temperatures can only be expected if the quantum mechanical nature of the ionic motion is taken into account, e.g., only quantum-mechanical calculations result in a vanishing volume expansion coefficient near absolute zero. In the vicinity of the phase transition, such quantum effects do not play a role and will not be considered in the following.

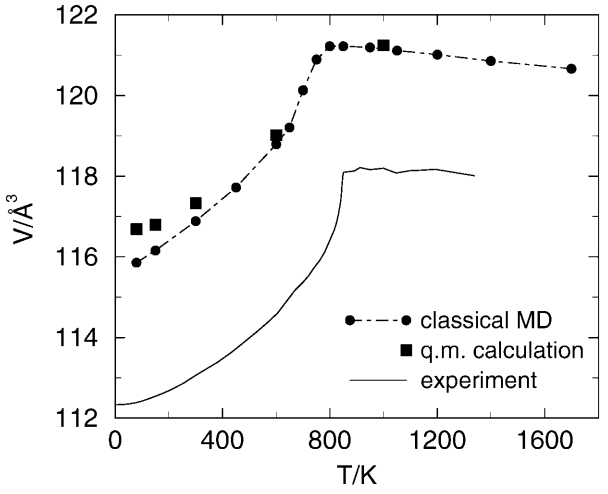

Fig. 1 Volume V per unit cell of quartz as a function of temperature T. Classical molecular dynamics simulation, path integral molecular dynamics (quantum-mechanical calculations) and experimental data (Carpenter et al. 1998) are shown

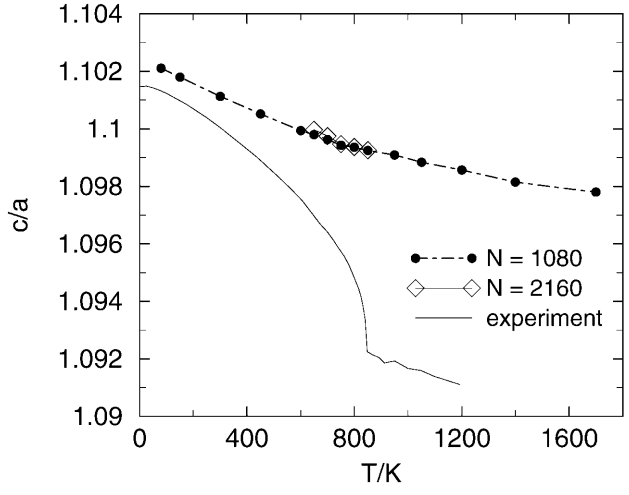

Fig. 2 c/a ratio of quartz as a function of temperature T. Two different system sizes are considered. *Solid lines* correspond to experimental data. (Carpenter et al. 1998)

It is striking that the volume jump seen in the simulations is much less pronounced than in experiment. This discrepancy can be understood if the c/a ratio is calculated. Unlike experiment, no discontinuity in the c/a ratio is observed in the simulations as shown in Fig. 2. By considering different system sizes, it is possible to rule out finite-size effects as the reason for the missing discontinuity in the simulation. The same discrepancy between simulation and experiment is obtained when the TTAM potential is used instead of the BKS potential, which has been checked for some representative data points. Unfortunately, this observation has not yet been made public in other MDS studies of this transition known to us. Since both the TTAM potential and the BKS potential are two-body potentials, one may speculate that the qualitative discrepancy between simulations and experiments could be remedied if three-body forces were employed. Despite the qualitative difference in the c/a behavior, a meaningful interpretation of experimental results with the help of simulations can still be possible. The main effect is a renormalization of the effective coefficients describing the free energy as a function of ϕ.

Despite the fact that computer simulation results for elastic constants at nonzero temperature are plagued with large statistical

uncertainties, qualitative agreement between calculated and experimentally observed elastic constants can be found, as shown in Fig. 3. In particular, the strong temperature dependences near T_{tr} are similar, although the transition temperatures T_{tr} differ by about 100 K between simulation ($N = 1080$) and experiment. It is interesting to note that the elastic constants at $T = 0$ K correspond very closely to the experimental data at $T = 300$ K while the agreement is less good for the $T = 300$ K simulations. This is, of course, a consequence of the way in which the model potential parameters were determined: ab initio data along with elastic modulii measured experimentally at $T = 300$ K were used to construct a potential energy surface such that the calculated classical zero-temperature elastic constants agreed with the finite-temperature experimental data. Nonetheless, the experimental features are well reflected, e.g., C_{11} and C_{33} cross between high and low temperatures similar to C_{44} and C_{66} (both shown in Fig. 3a), while C_{13} and C_{14} do not cross. For symmetry reasons, C_{14} vanishes in β-quartz. Thus, the slightly nonzero values for $T > T_{tr}$ shown in Fig. 3b reflect the statistical uncertainties of our calculations.

Finite-size effects and comparison to Landau theory

As a next step, we are concerned with the characteristics related to the order parameter. First, it is necessary to calculate the transition temperature, T_{tr}. It is difficult to locate T_{tr} precisely by just calculating the expectation value of the (absolute value) of ϕ, because all thermodynamic properties behave smoothly for finite-size systems near the phase transition temperature. In order to determine the transition temperature T_{tr} nevertheless accurately, use is made of the fourth order cumulant (Binder 1981), which is defined in the case of a one-component order parameter as

$$g_4(N,T) = \frac{1}{2}\left(3 - \frac{\langle\phi^4\rangle_N}{\langle\phi^2\rangle_N^2}\right) \ , \tag{2}$$

where $\langle\phi^k\rangle_N$ denotes the thermal average of the k'th moment of the order parameter for an N-particle system. It has been shown (Vollmayr et al. 1993) that $g_4(N,T)$, aside from small correction terms, has a size-independent crossing point g_4^* at a first-order phase transition. For the calculation of g_4^*, the geometry of the simulation cell is supposed to be constant. It is difficult to satisfy this requirement without increasing the particle number N considerably for the quartz structure if the cell geometries are approximately cubic. The smallest box length should exceed twice the cutoff radius, which limits us to $N \geq 1080$. While it is still possible to equilibrate system sizes of the order $N \approx 2000$ near the phase transition, this becomes extremely difficult for $N \approx 4000$. Note that the equilibration time increases algebraically with N at a second-order and exponentially with N at a first-order transition point.

The expectation values of the cumulants are shown in Fig. 4. Due to the fact that the cell geometry slightly differs between the $N = 1080$ and the $N = 2160$ system, we cannot expect perfect crossing of the two different systems at T_{tr}. However, comparison with the value where the cumulants cross in a Landau description of this transition (see below for more details) makes it plausible that the crossing of the cumulants shown in Fig. 4 is indeed meaningful. Within the statistical error bars, it is possible to locate the transition at $T_{tr} \approx 740$ K with an uncertainty of about 5 K for both system sizes.

In order to describe the transition within a Landau theory with a single scalar order parameter, we adopt the form (Carpenter et al. 1998; Bachheimer and Dolino 1975; Banda et al. 1975; Grimm and Dorner 1975)

$$F(\phi,T) = \frac{1}{2}a(T - T_c)\phi^2 + \frac{1}{4}b\phi^4 + \frac{1}{6}c\phi^6 \ , \tag{3}$$

where F is the free energy per particle as a function of temperature T and order parameter ϕ while a, b, c, and T_c are (free) parameters. In order to find those parameters that are appropriate to describe our simulation results, we need to generalize the approach to *finite* system sizes. This is done by evaluating numerically expectation

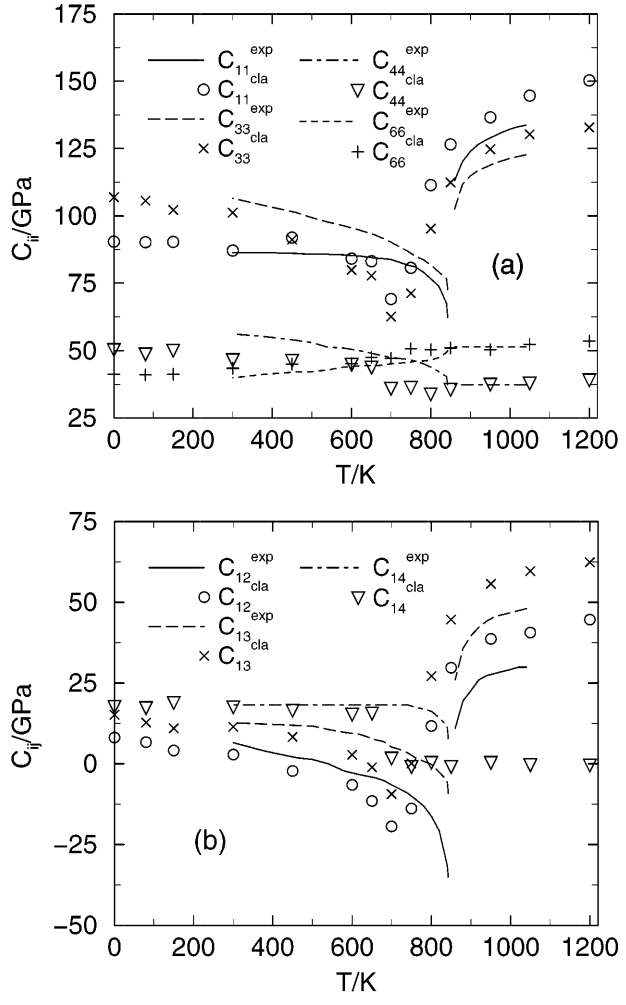

Fig. 3a, b Elastic constants as a function of temperature. *Solid lines* show experimental data accumulated in Carpenter et al. (1998). *Symbols* show simulation results. **a** C_{11}, C_{33}, C_{44}, C_{66} **b** C_{12}, C_{13}, C_{14}

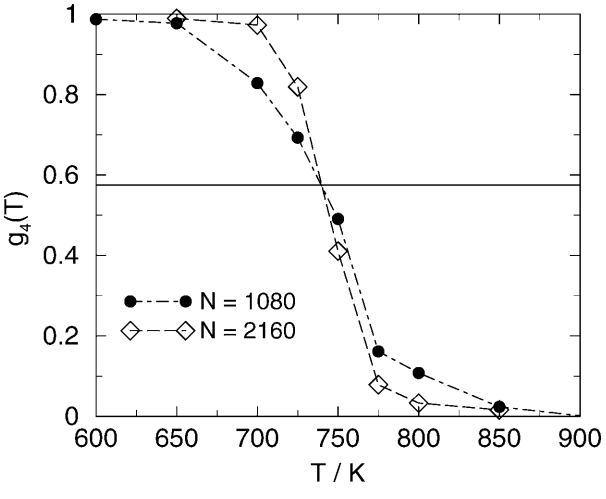

Fig. 4 Fourth-order cumulant g_4 as a function of temperature T for two different system sizes. The value g_4^* at which crossing of the cumulants is predicted within Landau theory is indicated by a *straight line*. *Broken lines* are drawn to guide the eye

values of the n'th power of ϕ using ($\beta = 1/k_B T$) in the following way:

$$\langle \phi^n \rangle = \frac{\int_{-\infty}^{\infty} \mathrm{d}\phi \phi^n \exp\{-\beta N F(\phi, T)\}}{\int_{-\infty}^{\infty} \mathrm{d}\phi \exp\{-\beta N F(\phi, T)\}} \quad . \tag{4}$$

The parameters a, b, c, and T_c were determined by fitting the temperature dependence of the order parameter $\langle|\phi|\rangle$ for the $N = 1080$ system. The fit is shown in Fig. 5 along with similar data for $N = 2160$. We also included data in which the thermodynamic limit was taken. It can be seen that the size effect in $\langle|\phi|\rangle$ is reasonably described by Landau theory.

Experimentally, susceptibilities χ have been reported only above T_{tr} (Carpenter et al. 1998). Within linear response theory, χ is the proportionality factor between order parameter ϕ and an external field that couples to ϕ; for example, in the case of a magnetic response $\langle M \rangle = \chi h$, with $\langle M \rangle$ the magnetization (order parameter) and h the magnetic field. χ can also be determined from thermal equilibrium fluctuations of ϕ. Experimentally, the measurement of χ associated with the order parameter describing the α–β transition in quartz can only be done indirectly.

Here, we try to fill the gap for $T < T_{tr}$ and check whether the Landau description is also appropriate for the calculation of χ. For finite systems, χ can be defined as:

$$\chi_N(T) = \frac{N}{k_B T} \times \begin{cases} \langle \phi^2 \rangle & \text{for } g_4 \le g_4^* \\ \langle \phi^2 \rangle - \langle |\phi| \rangle^2 & \text{for } g_4 > g_4^* \end{cases} \quad . \tag{5}$$

This definition of χ_N gives the proper value of χ in the thermodynamical limit $N \to \infty$. Results are shown in Fig. 6, where predictions from Landau theory are inserted as well. Again, the agreement is reasonable but less satisfying than for the order parameter itself. In particular, at $T = 0$ K (not included in the graph), the susceptibilities are twice as large in Landau theory compared to the simulation. Of course, Landau theory cannot be expected to hold down to $T = 0$ without terms of still higher order. Near the transition, however, the agreement is fairly reasonable. The good agreement between the $N = 2160$ data and the Landau theory for the thermodynamic limit at temperatures $T \le 725$ can be explained by the observation that no crossing of the free-energy barrier to the disordered state took place in the $N = 2160$ system. These transitions are extremely infrequent, but their effect on χ is very large.

Overall, coefficients similar to those from experimental data are drawn from the simulations. Most importantly, the parameter b is found to be slightly negative, $T_c = 715$ K is obtained about 115 K smaller than in experiment, and T_t–$T_c \approx 20$ K is found about twice as large as in real experiment (Carpenter et al. 1998). Nonetheless, the global picture of experiment is certainly reproduced.

Local structure in quartz near the phase transformation

Now, where we have established that the transition is reflected well by our model system, we want to gain insight into the local structure, in particular of the high-temperature phase. In order to do this, we calculate the radial distribution functions $g_{SiSi}(r)$, $g_{SiO}(r)$, and $g_{OO}(r)$. As is well known, molecular dynamics simulations can obtain all these three radial distribution functions individually in a straightforward way and with very good accuracy, and thus complement experiments where this information is not easily available. While the peaks in $g(r)$ related to neighboring Si–Si, Si–O, or O–O evolve rather smoothly as the temperature is lowered, many other peaks show abrupt changes as T becomes smaller than T_{tr}, which was found to be $T_{tr} = 740 \pm 5$ K in our model system. Some effects in $g(r)$ are shown exemplarily for some selected areas of the radial distribution functions in Fig. 7. A description of the radial distribution functions over a much wider range of distances at two temperatures far off from T_{tr} is given in Fig. 8.

The local structures in β-quartz can certainly not be interpreted as (temperature) broadened α-quartz domains, e.g., there are clear double peaks in g_{SiSi} at $r \approx 5.6$ Å and g_{SiO} at $r \approx 6.25$ Å in the α phase that are absent in the β phase. The various $g(r)$s do not change significantly with temperature above T_{tr}, but make sudden changes near and below T_{tr}. The (double) peaks in $g(r)$ become increasingly more pronounced as the temperature is lowered further below T_{tr}. It is important to note that there are strong hysteresis effects in $g(r)$ for large systems. The configurations in Fig. 7 at $T = 750$ K have been equilibrated for 3000 MD steps before the

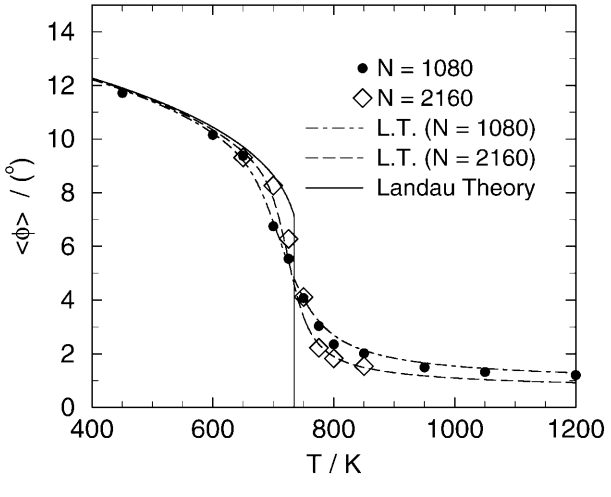

Fig. 5 Order parameter $\langle|\phi|\rangle$ as a function of temperature. The *lines* reflect fits according to Landau theory, whose free parameters were adjusted to the $N = 1080$ curve. The *solid line* corresponds to the thermodynamic limit in Landau theory; *broken lines* represent finite-size Landau theory

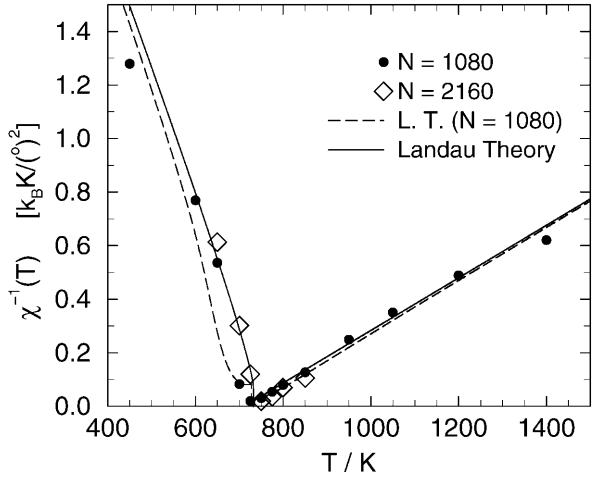

Fig. 6 Inverse susceptibility χ^{-1} (per atom) as a function of temperature T for two different system sizes. The *lines* reflect Landau theory

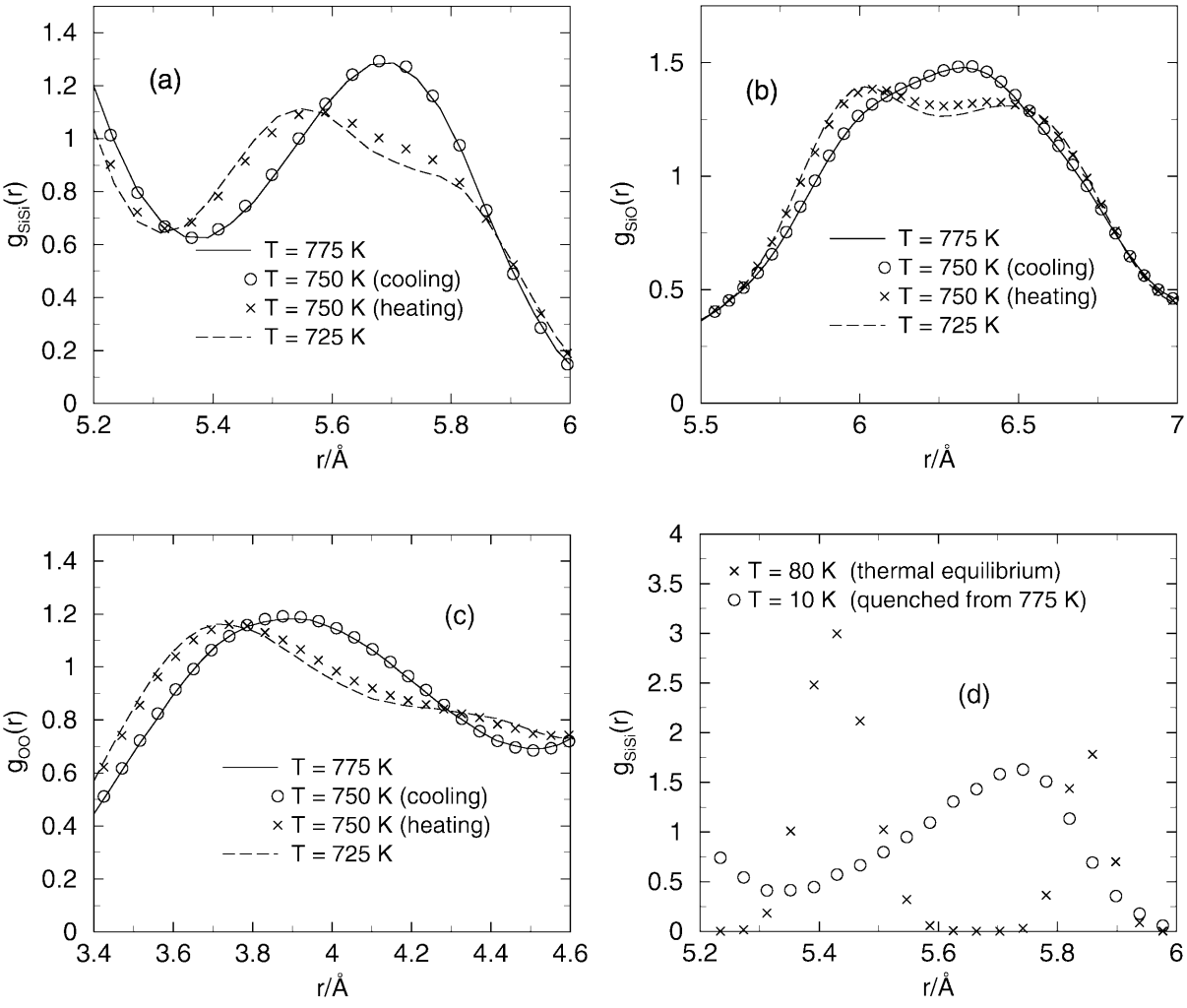

Fig. 7a–d Details of the radial distribution function Si–Si **a**, Si–O **b**, and O–O **c** for system size $N = 4320$ at various temperatures. **d** is same as **a**, but from configurations that have been quenched from high-temperature phase to 10 K

radial distribution functions were averaged over 2000 MD steps. The initial configurations were equilibrated configurations from 25 K below or above 750 K. Smaller systems, e.g., $N = 1080$ systems, relax considerably at $T = 750$ K within the above-mentioned equilibration time period. It is striking that no double peak in the SiSi radial distribution function is observed when $T = 750$ K configurations are quenched down to $T = 10$ K (Fig. 7d). Quenching is realized by suddenly dropping the temperature and choosing much larger couplings to the thermostat than usual. The quenching simulations show that there are no α_1 and α_2 domains 35 K above T_{tr}.

While this paper was under review, an experimental study was published with similar conclusions: Tucker et al. (2000) deduced the nearest-neighbor Si–Si–Si angle distribution from the so-called total pair correlation function $T(r)$. They found that two peaks of the Si–Si–Si angle distribution coalesced upon heating at the α–β phase transition. This finding corresponds to the behavior shown in Fig. 7a and d. Our simulations suggest additionally that the splitting is even larger for nearest-neighbor O–O–O angle distributions, see Fig. 7c.

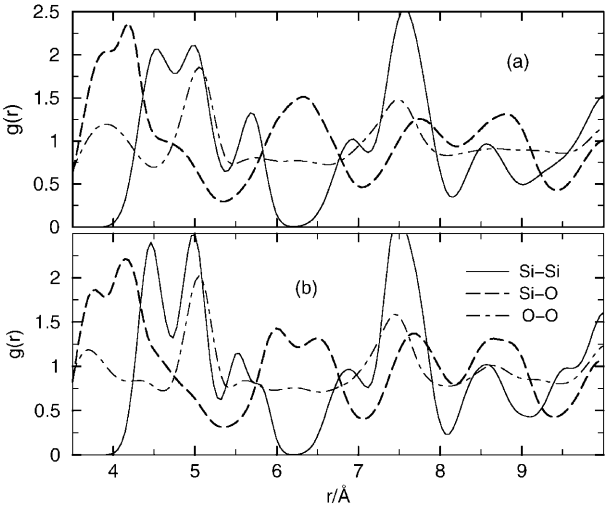

Fig. 8a, b Radial distribution functions for 3.5 Å $< r <$ 10.0 Å at temperatures $T = 875$ K **a** and $T = 625$ K **b**

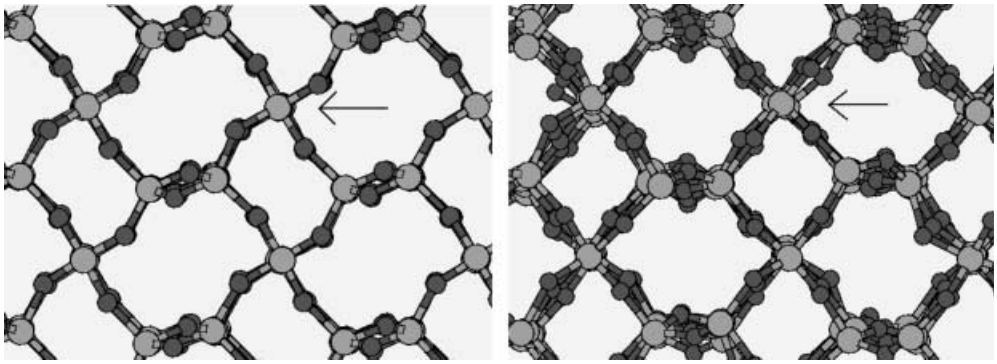

Fig. 9 View along the [1 0 0] axis in α-quartz at $T = 80$ K (*left*) and β-quartz at $T = 1050$ K (*right*). *Dark and light atoms* represent oxygen and silicon atoms, respectively. Both snapshots belong to identical subvolumes of the simulation cell. The [0 0 1] axis goes *from the left to the right*. The rotation angles about the [1 0 0] axis of the units marked by an *arrow* are used to define the order parameter

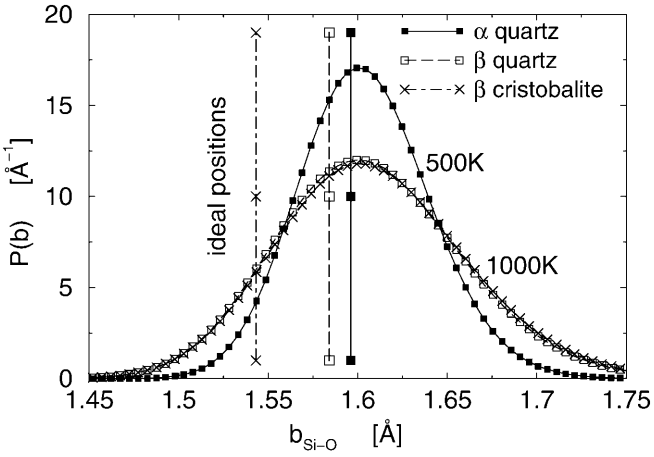

Fig. 10 Probabilty $p(b)$ to find an oxygen atom a distance b away from a silicon atom. β-quartz and β-cristobalite simulations were carried out at $T = 1000$ K, those for α-quartz at 500 K. The *straight lines* reflect the location of the Si–O bond lengths as deduced from the average structure

It is instructive to visualize the changes of the structure in quartz. This is done in Fig. 9, where a snapshot along the [1 0 0] axis is taken for α-quartz at $T = 80$ K and for β-quartz at $T = 1050$ K. The rotation of tetrahedra about the [1 0 0] axis can be seen particularly well for the positions that are equivalent to those sites marked by an arrow. In the β-quartz phase, no α_1 or α_2 domains become apparent. This statement also holds for most configurations obtained near but above T_{tr}. For large system sizes near T_{tr}, it is actually possible to observe jumps of the entire system between configurations that entirely resemble the α-quartz structure and those that resemble β-quartz.

Nevertheless, even in the high-temperature phase, the local geometry is seldomly close to the β-quartz structure. By averaging the structure over different time scales, we observe the following phenomena at $T =$ 900 K (160 K above "our" phase transition temperature): Snapshots of the configuration look very much like the right-hand side of Fig. 9. When averaged over about 300 MDS, which corresponds to a time interval of about 0.4 ns, the local α-quartz order parameter is basically identical to zero, but the average positions of the oxygens have not yet relaxed onto their ideal positions! Hence, the ideal β-quartz positions do not correspond to the positions around which the oxygen atoms actually fluctuate. When the configurations were averaged over about 4 ns, the averaged oxygen positions were close to the ideal oxygen positions of β-quartz.

An indication for the fluctuations about the average positions being anharmonic is obtained from the bond-length distribution function. For β-cristobalite, it has been shown experimentally that the real bond-length distribution function peaks at a radius that is distinctly larger than the bond length deduced from the average structure (Dove et al. 1997). This effect is less strong in β-quartz, as shown in Fig. 10. Yet, it is clear that the tendencies in β-cristobalite and β-quartz are similar: the Si–O bond lengths deduced from the average structures are located at a position that is markedly smaller than the position where the bond-length distribution peaks. The bond lengths from the average positions shown in Fig. 10 are deduced from our simulation. The values we obtain for β-cristobalite agree well with those suggested by Dove et al. (1997). They state that the bond length of the average position is about 1.55 Å, while their bond length distribution peaks at 1.61–1.62 Å. There is also qualitative agreement of our simulations with experimental data on β-quartz: Kihara (1990) reported a real SiO bond length of 1.62 Å, which is about 0.04 Å larger than the spectroscopic bond length of 1.588 Å, while our simulations suggest a change of only 0.02 Å. A recent neutron diffraction study confirms Kihara's results quite accurately (Tucker et al. 2000).

The delocalization of the oxygen atoms is also illustrated in Fig. 11, where the probability $p(r)$ to find an atom a distance r away from its average position (with respect to the center of mass of the simulation box) divided by r^2 is shown as a function of r. For the Si atoms, a single Gaussian is obtained, while the O atoms apparently have several preferred sites, which is obvious from the anomaly in the $p(r)/r^2$ curve. These results strongly support the X-ray study by Kihara (1990) in which the oxygen pdf's were conjectured to deviate

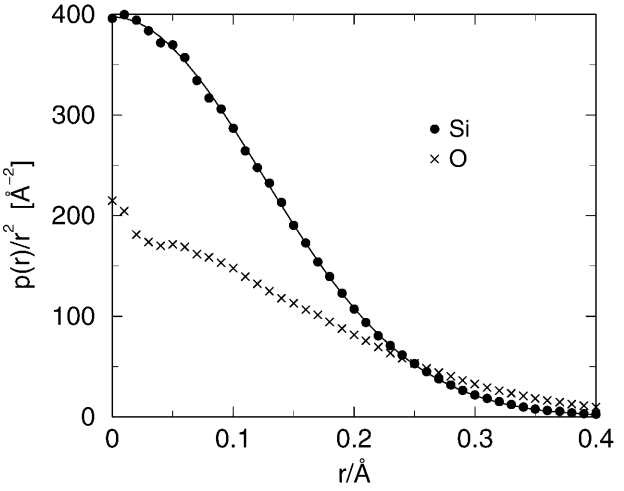

Fig. 11 Probabilty $p(r)$ to find an atom a distance r away from its average position (with respect to the center of mass of the simulation box) divided by r^2 as a function of r. *Circles* refer to Si atoms, *crosses* to O atoms. The *straight line* is a Gaussian fit through the Si data. $T = 900$ K

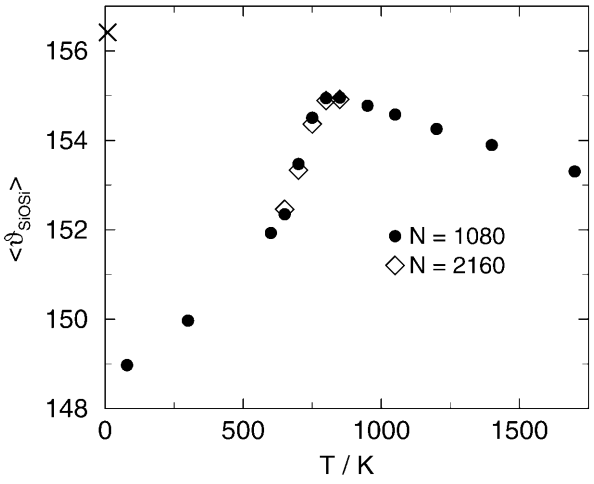

Fig. 12 Average Si–O–Si bond angle $\langle\vartheta_{\mathrm{SiOSi}}\rangle$ as a function of temperature T. The *cross* indicates a simulation where an equilibrated $T = 775$ K system was quenched down to $T = 10$ K

considerably from Gaussians. Kihara (1990) examined the pdf's in further detail: the largest principal axis of the ellipsoid representing the pdf did not coincide with the vector connecting the α_1 and α_2 positions but deviated toward the vector that is normal to the Si–O–Si plane. This observation is also fully supported by our simulations. The analysis of pdf's alone, however, does not enable us to exclude the presence of small α-quartz domains in β-quartz. This is why we concentrate on the Si–Si radial distribution function $g_{\mathrm{SiSi}}(r)$, which is discussed above.

Further evidence for the claim that the ideal β-quartz structure is not a typical "reference" structure of the β phase can be obtained by quenching the system from $T > T_{\mathrm{tr}}$ to extremely small temperatures. A system is quenched by suddenly dropping the temperature to $T = 10$ K and increasing the coupling to the thermostat by a factor of 10. After a considerable amount of relaxation, the local order parameters still remain close to zero, but the oxygen atoms do not relax to their ideal positions.

The local quantity that maybe differs most dramatically between the average (spectroscopic) structure and the real structure is the SiOSi bond angle, $\vartheta_{\mathrm{SiOSi}}$. The average value of $\vartheta_{\mathrm{SiOSi}}$ is close to the value that is obtained if β-quartz is quenched to small temperatures, but it is strikingly different from $\vartheta_{\mathrm{SiOSi}}$ obtained from the average/spectroscopic atomic positions. $\langle\vartheta_{\mathrm{SiOSi}}\rangle$ is shown as a function of temperature in Fig. 12. Note that the value of $\vartheta_{\mathrm{SiOSi}}$ evaluated for the average or ideal structure is significantly larger, namely $\vartheta_{\mathrm{SiOSi}}^{(\mathrm{ideal})} = 159.2$ for $T = 1000$ K as compared to $\langle\vartheta_{\mathrm{SiOSi}}\rangle = 154.6$. This result is again in qualitative agreement with the experimental results by Kihara (1990), who suggested a value of $\vartheta_{\mathrm{SiOSi}}^{(\mathrm{ideal})} = 153.4$ as compared to $\langle\vartheta_{\mathrm{SiOSi}}\rangle = 144.2$. We wish to note that we do not observe a dramatic discontinuity in $\langle\vartheta_{\mathrm{SiOSi}}\rangle$ at the transition in the simulations.

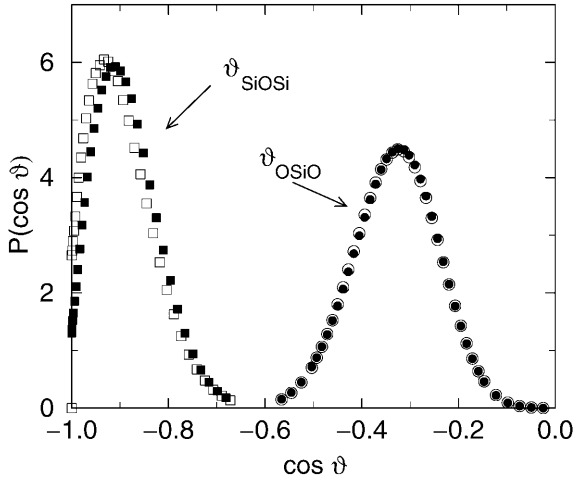

Fig. 13 Bond angle distribution function for an $N = 4192$ system at $T = 750$ K with different thermal histories. *Filled symbols* refer to heating simulations while *open symbols* refer to cooling simulations. Both systems were equilibrated for 3000 MD steps before the distribution was accumulated

It is interesting to note that the bond angle distributions on either side of the phase transition are similar, although a small sudden change in the $\vartheta_{\mathrm{SiOSi}}$ distribution can be observed. This is shown in Fig. 13. Again, we consider the $N = 4192$ system, which can be held stable at $T = 750$ K in either phase for a sufficiently long time to analyze structural properties in detail. The distribution of the bond angle $\vartheta_{\mathrm{OSiO}}$, however, is nearly identical for both symmetries. This observation indicates that the SiO_4 units basically do not distort at the transition. Consequently, SiO_4 units are already distorted in the β-quartz phase. This statement also holds for temperatures far away from T_{tr}. A comparison of our data with the data of Kihara (1990, Table 6) cannot be made here, as we have not recorded O–Si–O bond angles individually.

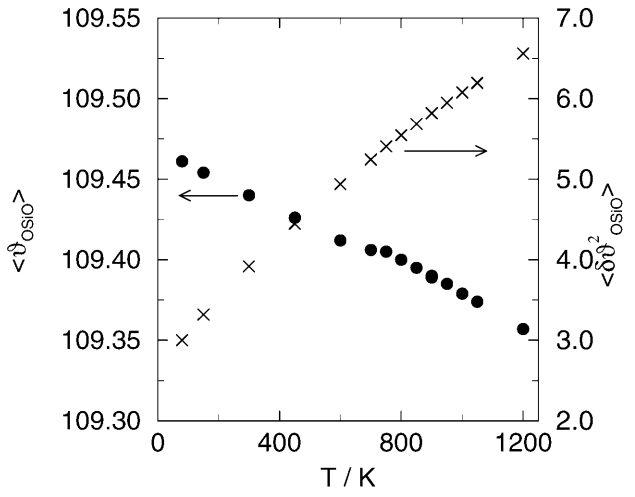

Fig. 14 Average O–Si–O bond angle $\langle\vartheta_{\mathrm{OSiO}}\rangle$ (*circles*, *left* *y*-axis) as well as its second moment $\langle\delta\vartheta^2_{\mathrm{OSiO}}\rangle$ (*crosses*, *right* *y*-axis) as a function of temperature T

The discontinuities in the Si–0 bond length and the *average* O–Si–O bond angles show much smaller effects near the α–β transition than $\vartheta_{\mathrm{SiOSi}}$. We show exemplarily the temperature dependence of the average O–Si–O bond angle $\langle\vartheta_{\mathrm{OSiO}}\rangle$ as well as the second moment of the $\langle\delta\vartheta^2_{\mathrm{OSiO}}\rangle$ in Fig. 14.

The observation that the local structure in β-quartz is not similar to the ideal β-quartz structure has serious implications for the calculation of bulk properties, in particular, however, for the elastic modulii in the β phase: in the (NVT) ensemble, correct elastic constants are obtained by taking the second derivative of the expectation value of the potential energy with respect to the strain tensor around the actual, thermal positions minus a term related to fluctuations of the stress plus small corrections due to the ideal gas behavior (Squire et al. 1969). Hence, elastic constants as well as all other thermomechanical data evaluated around ideal β-quartz positions are not necessarily related to the properties which one would obtain if thermal fluctuations were taken into account properly, no matter how sophisticated the level of the ab initio treatment. Hence, the large overestimation of elastic modulii in the β-phase obtained by density functional theory methods (Demuth et al. 1999). Similarly, the overestimation of T_{tr} by (Gambhir et al. 1999) can be related to this observation: the potential energy of the β phase is always overestimated with respect to the one of the α phase. This, of course, leads to an overestimation of T_{tr}. Similar statements can be expected to hold for other properties and other crystalline high-temperature phases as well.

Summary

This molecular dynamics study shows to what extent two-body potentials like the BKS potential can be used to obtain qualitative information about the α–β phase transition in quartz. The transition temperature T_{tr} as well as the anomalies in the elastic constants can be reproduced in good agreement with experimental data. Like experimental data, the temperature dependence of the order parameter and the susceptibility can be interpreted in terms of a Landau theory for (weak) first-order transitions. It has been shown that also the susceptibilities below T_{tr} are in agreement with the Landau description, which has not yet been tested experimentally. However, the temperature regime in which Landau theory predicts the susceptibility accurately is considerably smaller than in the high-temperature phase. There is a qualitative difference between simulation and experiment, which is the absence of the anomaly in the c/a ratio at T_{tr} in the simulations. This could be due to the absence of three-body interactions in the BKS potential.

Thorough analysis of the local order near T_{tr} shows that SiO_4 units are already considerably deformed in the β phase and do not deform significantly any further at the phase transition. The main effect is a (small) sudden change in the SiOSi bond angle distribution. This change can be made responsible for the large hysteresis effects observed in the local structure. In the β phase, we could identify two relaxation phenomena: (1) relaxation of the orientation of deformed tetrahedra and (2) relaxation of the oxygen atoms onto their ideal β-quartz positions. Process (1) takes place on relatively short time scales, e.g., 0.4 ns at $T = T_{\mathrm{tr}} + 140$ K, while process (2) is much slower. Due to process (1), the previous statement by Tsuneyuki et al. (1990) that β-quartz consists of small α_1 and α_2 domains which spatially and dynamically average to the β quartz structure domains could be ruled out. An important consequence of the relaxation process (2) is that the local β-quartz structure does not fluctuate around the ideal β-quartz structure. The oxygen atoms fluctuate around time-dependent equilibrium positions that average to the ideal β-quartz structure on time scales longer than 1 ns. This picture is in agreement with the observation of non-Gaussian oxygen probability density functions suggested by Kihara (1990). Unfortunately, ab initio studies and theoretical model building of high quartz or other high-silica polymorphs often ignore this effect, resulting in uncontrolled approximations for the high-quartz phase.

While this paper was in the reviewing process, Tucker et al. (2000) published a neutron scattering study probing simultaneously the local and the long-range structural order. Their study agrees well with our simulations, namely, the phase transition invokes a concurrent change in the long- and the short-range structural order. Thus, the disorder in β-quartz is unequivocally unrelated to a (hypothetical) coexistence of finite α_1 and α_2 domains in β-quartz above T_{tr}. The study by Kihara (1990) gave early and important hints to rule out the existence of such domains in β-quartz, the possibility of a weakly disordered model was yet still mentioned in the concluding remarks.

Acknowledgements Support from the BMBF through Grant 03N6015 and from the Materialwissenschaftliche Forschungszentrum Rheinland-Pfalz is gratefully acknowledged.

References

Axe JC, Shirane G (1970) Study of the α–β phase transformation by inelastic bneutron scattering. Phys Rev (B)1: 342–348

Bachheimer JP, Dolino G (1975) Measurement of the order parameter of α-quartz by second harmonic generation of light. Phys Rev (B)11: 3195–3205

Banda EJ, Craven RA, Parks RD, Horn PM, Blume M (1975) α–β transition in quartz: classical versus critical behaviour. Solid State Commun 17: 11–14

Binder K (1981) Critical properties from Monte Carlo: coarse graining and renormalization. Phys Rev Lett 47: 693–696

Binder K, Stauffer D (1987) In: Binder k (ed.), Applications of the Monte Carlo method in statistical physics. Springer, Berlin Heidelberg New York

Binggeli N, Chelikowsky JR (1992) Elastic instability in α-quartz under pressure. Phys Rev Lett 69: 2220–2223

Carpenter MA, Salje EKH, Graeme-Barber A, Wrucki B, Dove MT, Knight KS (1998) Calibration of excess thermodynamic properties and elastic constant variations associated with the $\alpha \leftrightarrow \beta$ phase transition in quartz. Am Mineral 83: 2–22

Cowley RA, Bruce AD (1980) Structural phase transitions. Adv Phys 29: 1–320

Demuth T, Jeanvoine Y, Hafner J. Angyan JG (1999) Polymorphism in silica studied in the local density and generalized-gradient approximation. J Phys Condens Matt 11: 3833–3874

Dolino G (1990) The α-inc-β phase transition of quartz: a century of research on displacive phase transitions. Phase Trans 21: 59–72

Dove MT, Kreen DA, Hannon AC, Swainson IP (1997) Direct measurement of the Si–O bond length and orientational disorder in the high-temperature phase of cristobalite. Phys Chem Miner 24: 311–317

Dove MT, Gambhir M, Heine V (1999) Anatomy of a structural phase transition: theoretical analysis of the displacive phase transition in quartz and other silicates. Phys Chem Miner 26: 344–353

Gambhir M, Dove MT, Heine V (1999) Rigid unit modes and dynamic disorder: SiO_2 cristobalite and quartz. Phys Chem Miner 26: 484–495

Gregoryanz E, Hemley RJ, Mao HK, Gillet P (2000) High-pressure elasticity of α-quartz: instability and ferroelastic transition. Phys Rev Lett 84: 3117–3120

Grimm H, Dorner B (1975) On the mechanism of the α–β transformation in quartz. J Phys Chem Solids 36: 407–413

Heaney PJ, Prewitt CT, Gibbs GV (eds) (1994) Silica. Physical behavior, geochemistry, and materials applications. Mineralogical Society of America, Washington, DC

Kihara K (1990) An X-ray study of the temperature dependence of the quartz structure. Eur J Miner 2: 63–77

Müser MH (2001) Simulation of material properties below the Debye temperature: a path-integral molecular dynamics case study of quartz. J Chem Phys 114: 6364–637

Parrinello M, Rahman A (1980) Crystal structure and pair potentials: a molecular-dynamics study. Phys Rev Lett 45: 1196–1199

Parrinello M, Rahman A (1982) Strain fluctuations and elastic constants. J Chem Phys 76: 2662–2666

Salje EKH, Ridgwell A, Güttler B, Wruck B, Dove MT, Dolino G (1992) On the displacive character of the phase transition in quartz: a hard mode spectroscopic study. J Phys Condens Matt 4: 571–577

Spearing DR, Farnan I, Stebbins JF (1992) Dynamics of the α–β transition in quartz and cristobalite as observed by in-situ high temperature ^{29}Si and ^{17}O NMR. Phys Chem Miner 19: 307–321

Squire DR, Holt AC, Hoover WG (1969) Isothermal elastic constants for argon: theory and Monte Carlo calculations. Physica 42: 388–397

Tezuka Y, Shin S, Ishigame M (1991) Observation of the silent soft phonon in β-quartz by means of hyper-Raman scattering. Phys Rev Lett 66: 2356–2359

Tse JS, Klug DD (1991) The structure and dynamics of silica polymorphs using a two-body effective potential. J Chem Phys 95: 9176–9185

Tsuneyuki S, Tsukada M, Aoki H, Matsui Y (1988) First principles interatomic potential of silica applied to molecular dynamics. Phys Rev Lett 61: 869–872

Tsuneyuki S, Aoki H, Tsukada M (1990) Molecular-dynamics study of the α to β structural phase transition in quartz. Phys Rev Lett 64: 776–779

Tucker MG, Dove MT, Keen, DA (2000) Simultaneous analysis of changes in long-range and short-range structural order at the displacive phase transition in quartz. J Phys Condens Matt 12: L723–L730

van Beest BWH, Kramer G, van Santen R (1990) Force fields for silicas and aluminophosphates based on ab initio calculations Phys Rev Lett 64: 1955–1958

Vollmayr K, Reger JD, Scheucher M, Binder K (1993) Finite size effects at thermally driven first-order phase transitions: a phenomenological theory of the order parameter distribution. Z Phys (B) 91: 113

Wright AF, Lehmann MS (1981) The structure of quartz at 25 and 590 °C determined by neutron diffraction. J Solid State Chem 36: 372–380